PHYSICAL REVIEW D **87,** 064008 (2013)

Metric perturbations from eccentric orbits on a Schwarzschild black hole. I. Odd-parity Regge-Wheeler to Lorenz gauge transformation and two new methods to circumvent the Gibbs phenomenon

Seth Hopper*
Max-Planck-Institut für Gravitationsphysik, Albert-Einstein-Institut, Am Mühlenberg 1, D-14476 Golm, Germany

Charles R. Evans†
Department of Physics and Astronomy, University of North Carolina, Chapel Hill, North Carolina 27599, USA
(Received 6 November 2012; published 6 March 2013)

We calculate the odd-parity, radiative ($\ell \geq 2$) parts of the metric perturbation in Lorenz gauge caused by a small compact object in eccentric orbit about a Schwarzschild black hole. The Lorenz gauge solution is found via gauge transformation from a corresponding one in Regge-Wheeler gauge. Like the Regge-Wheeler gauge solution itself, the gauge generator is computed in the frequency domain and transferred to the time domain. The wave equation for the gauge generator has a source with a compact, moving delta-function term and a discontinuous noncompact term. The former term allows the method of extended homogeneous solutions to be applied (which circumvents the Gibbs phenomenon). The latter has required the development of new means to use frequency domain methods and yet be able to transfer to the time domain while avoiding Gibbs problems. Two new methods are developed to achieve this: a partial annihilator method and a method of extended particular solutions. We detail these methods and show their application in calculating the odd-parity gauge generator and Lorenz gauge metric perturbations. A subsequent paper will apply these methods to the harder task of computing the even-parity parts of the gauge generator.

DOI: 10.1103/PhysRevD.87.064008 PACS numbers: 04.25.dg, 04.30.−w, 04.25.Nx, 04.30.Db

I. INTRODUCTION

The increasing maturity of space-based gravitational wave detector concepts [1,2] has in part motivated considerable work in the last fifteen years on self-consistent calculations of extreme-mass-ratio inspirals (EMRIs). Such a system consists of a small compact object of mass $\mu \simeq 1$–$10M_\odot$ (e.g., neutron star or black hole) moving on a decaying orbit about, and ultimately into, a supermassive black hole of mass $M \sim 10^5$–$10^9 M_\odot \gg \mu$. Irrespective of when a detector might launch, there is also simply considerable theoretical interest in the problem of motion of a point mass in a background geometry in general relativity, influenced by its own self-force [3].

The extreme mass ratio lends itself to use of black hole perturbation theory. In the limit of $\mu \to 0$, the small mass orbits on a geodesic of the massive black hole background with constants of motion. At next order the small mass draws up a small perturbation in the metric, which results in gravitational radiation fluxing to infinity and down the horizon of the massive black hole. The metric perturbation (MP) also acts back on the small body locally (through a self-force), giving rise to dissipative effects that cause the orbit to decay and to small conservative corrections to the motion. The perturbation problem is singular in several respects [4], with a divergence in the MP at the particle location making the motion correction also formally divergent. A general understanding of how to treat the self-force (i.e., regularize it) in an arbitrary spacetime was given by Mino *et al.* [5] and Quinn and Wald [6]. Practical procedures for regularizing the self-force in numerical calculations followed (e.g., Ref. [7]).

The physical retarded field $p^{\rm ret}_{\mu\nu}$ can be conveniently split into regular (R) and singular (S) parts, as first introduced by Detweiler and Whiting [8]. The advantage of this split is that while the singular contribution to the MP $p^S_{\mu\nu}$ satisfies the inhomogeneous field equations, it does not contribute at all to the self-force. On the other hand, the regular contribution, $p^R_{\mu\nu}$, is a smooth, homogeneous solution to the field equations and, through a projected gradient, is entirely responsible for the self-force. Indeed, when interpreted this way, the regular field can be thought of as an external field which sources the deviation from geodesic motion on the background metric $g_{\mu\nu}$. The motion of the particle is then geodesic on the spacetime $g_{\mu\nu} + p^R_{\mu\nu}$. The singular part of the MP is calculated analytically in Lorenz gauge, and an expansion provides the regularization parameters [7]. The singular part is then subtracted from the full retarded field mode by mode in a spherical harmonic expansion, allowing the difference $(p^R_{\mu\nu})$ to converge. While in principle [9,10] the full retarded field could be calculated in a variety of gauges, in practice most calculations [11–13] have also used Lorenz gauge to find $p^{\rm ret}_{\mu\nu}$.

*seth.hopper@aei.mpg.de
†evans@physics.unc.edu

We are developing a set of techniques and assembling a computer code to calculate with high accuracy the first-order MPs from a small compact object in a generic orbit about a Schwarzschild black hole. The need for high accuracy is related to a set of arguments that have been made for years that EMRIs should be calculated through second order in perturbation theory [3,14–17]. One particular argument centers on calculating the phase evolution of an EMRI and using it in interpreting data from a detector. For a small mass ratio $\epsilon = \mu/M$ (and in the absence of transient resonances [18] which may occur during EMRI evolution on a Kerr black hole), we expect that as an EMRI evolves through a detector passband, the gravitational waveform will accumulate (schematically) a phase of

$$\Phi = \kappa_1 \frac{1}{\epsilon} + \kappa_2 \epsilon^0 + \kappa_3 \epsilon^1 + \cdots, \tag{1.1}$$

where the κ's are coefficients of order unity that depend upon, among other things, the lower and upper limits in frequency of the detector response. The first term reflects the dissipative effects of the first-order self-force in spurring a decay of the orbit. The second term would result from second order in perturbation theory. For example, with $\epsilon = 10^{-6}$, an EMRI might be observed to accumulate a total phase of $\Phi \sim 10^6$. For matched filtering purposes we might need to compute the phase to an accuracy $\delta\Phi \lesssim 0.1$ and thus a fractional error of $\lesssim 10^{-7}$. However, the error in phase in using the first-order calculation alone is $\sim\mathcal{O}(1)$. Hence, the need for a second approximation to take full advantage of a detector output. However, there is a corollary to this argument. We cannot possibly hope to make use of a second-order calculation if we have not already computed the first-order self-force to a relative accuracy much better than $\mathcal{O}(\epsilon)$. The requirement might be at least several orders of magnitude better than $\mathcal{O}(\epsilon)$ to make a second order calculation worthwhile (say 10^{-9} to 10^{-8} in the example). Furthermore, given that computation of the self-force is a numerically subtractive procedure, the first-order preregularization field contributions likely need to be known even more accurately (perhaps 10^{-11} to 10^{-10}).

An accurate calculation strongly suggests use of Fourier decomposition and frequency domain (FD) methods to gain the benefit of integrating ordinary differential equations. Ultimately we are interested in the time-dependent self-force and must transfer back to the time domain (TD). For that step, a lynchpin of the effort has been use of the recently developed method of extended homogeneous solutions (EHS) [19], which allows partial Fourier series sums for the perturbations to avoid the Gibbs phenomenon and to converge exponentially even at the location of the point mass and despite loss of differentiability there. This conclusion has guided others as well [20,21].

Like other recent calculations, we want to determine the first-order MP in Lorenz gauge. However, our approach is indirect. In an earlier paper [22], we calculated radiative modes ($\ell \geq 2$) of the MP in Regge-Wheeler (RW) gauge by applying EHS to solutions of the master equations of the Regge-Wheeler-Zerilli (RWZ) formalism and then determining the metric from the master functions. The new aspect of that work was being able to use FD techniques and nevertheless determine the metric amplitudes in the TD with accuracy right up to the location of the particle $r = r_p(t)$, an essential requirement for computing the self-force accurately. EHS works by recognizing that the solution of a master equation with a moving singular source (in the RWZ case, the source has both a delta function term and a derivative of delta function term) is a weak solution of the form $\Psi(t, r) = \Psi^+(t, r)\theta[r - r_p(t)] + \Psi^-(t, r)\theta[r_p(t) - r]$, where $\Psi^+(t, r)$ and $\Psi^-(t, r)$ are differentiable solutions to the source-free master equation. Ψ^+ and Ψ^- are in turn obtained as Fourier sums of properly normalized Fourier-harmonic modes that solve the source-free master equation in the FD. Since the functions in the separate Fourier sums are smooth everywhere, the lack of differentiability of Ψ is captured entirely by the θ functions. We can in turn then calculate the MPs from Ψ. The result, however, is in RW gauge. This paper, and a subsequent one, address the calculation of the infinitesimal gauge generator that transforms $p^{\mathrm{RW}}_{\mu\nu}$ in RW gauge to its counterpart $p^{\mathrm{L}}_{\mu\nu}$ in Lorenz gauge.

This paper is restricted to finding the odd-parity part of the gauge generator, which for each spherical harmonic mode has an amplitude that is a solution to a single inhomogeneous wave equation. While the wave equation is simple to express, what is more challenging is to find a way to generalize the underlying idea behind EHS to equations with noncompact source terms. A substantial part of this paper is devoted to laying out two new analytic/numerical methods [method of partial annihilators (PA) and method of extended particular solutions (EPS)] we have developed for solving differential equations of this type. We present results from each of these methods, including a comparison of the two, showing that they agree to a high accuracy. These techniques will play a central role in a subsequent paper where we present the more involved procedure, based on analysis by Sago *et al.* [23], for determining the even-parity parts of the RW-to-Lorenz gauge generator. The Sago *et al.* approach takes the gauge generator equations for even parity, which are most naturally expressed as a set of three coupled equations for the vector spherical harmonic amplitudes, and transforms them to an altered set of equations in terms of different amplitudes. The resulting equations are a hierarchical set of second-order equations, in which solutions to preceding steps in the hierarchy form source terms for subsequent steps. The result is a system of equations that, while containing more steps (amplitudes), lends itself to the immediate application of the techniques developed here.

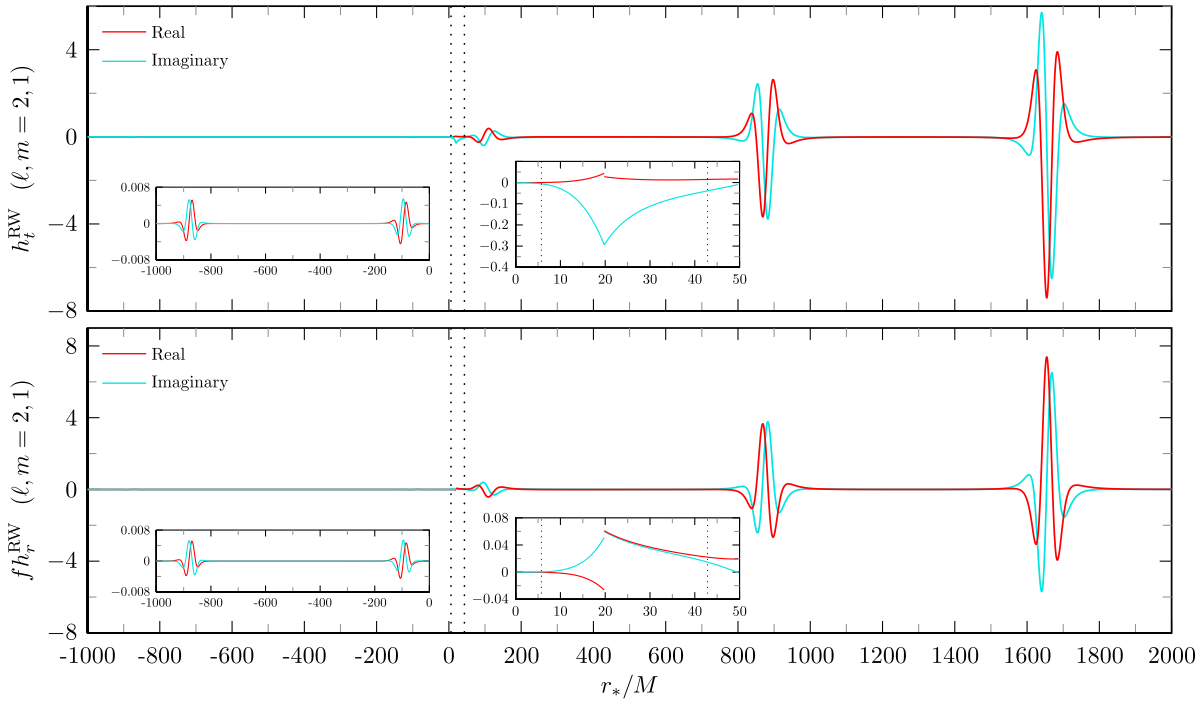

FIG. 1 (color online). The $\ell = 2$, $m = 1$ mode of the Regge-Wheeler gauge MP amplitudes $h_t^{\rm RW}$ and $h_r^{\rm RW}$. The orbit is parametrized by eccentricity $e = 0.764124$ and semilatus rectum $p = 8.75455$. The plots show the real and imaginary parts of the MP amplitudes at time $t = 93.58$ (where $t = 0$ is at the periapsis). Dotted vertical lines indicate limits of the source libration region. Insets show the discontinuities at the location of the particle. The lack of asymptotic flatness is evident as $r \to \infty$. We plot $f h_r^{\rm RW}$ so that the wave behavior near the horizon can be seen.

One might ask, why two new methods? In part, partial annihilators is the easier of the two methods to implement but requires that the partial annihilator operator be found. In some applications that may be difficult. In contrast, EPS is straightforward if somewhat more involved in terms of the number of steps. Ultimately, the main advantage of finding two methods is that they provide a powerful check on each other and confirmation that the solution has been obtained. We demonstrate this comparison in Sec. IV.

The discussion above begs the question, why the need to transform to Lorenz gauge? In part we know that the MP amplitudes in Lorenz gauge are C^0 in the TD at the particle location. As we discussed in Ref. [22] the MP amplitudes in RW gauge are one or two orders of continuity worse behaved (i.e., some amplitudes are C^{-1}, or discontinuous, and some have a delta function term at $r = r_p(t)$). Figure 1 demonstrates this problem graphically for the $\ell = 2$, $m = 1$ (odd parity) RW amplitudes $h_t^{2,1}$ and $h_r^{2,1}$. The insets show discontinuities in the MP amplitudes at the particle's location. The plots also show the $\propto r$ growth in the wave pulse amplitude as $r \to \infty$, reflecting the fact that RW gauge is not asymptotically flat [24]. Transformation to Lorenz gauge not only improves the behavior of the modes at $r = r_p(t)$, it also removes the nonasymptotically flat behavior seen in the radiative modes of RW gauge.

Lastly, we note that for nonradiative ($\ell = 0$, 1) modes, the RWZ formalism breaks down. Various researchers have used different gauges to solve the Einstein equations for these modes. Considering generic motion on a Schwarzschild background, Zerilli [25] solved for these modes analytically in his own gauge which exhibits C^{-1} behavior for certain modes. For circular orbits Detweiler and Poisson [26] showed how to transform Zerilli's solutions to Lorenz gauge. Barack and Sago [13] solved the Lorenz gauge field equations directly for these modes (and higher radiative modes). The nonradiative modes provide a crucial contribution to the conservative piece of the self-force. In this paper, though, we are solely concerned with transforming our RW gauge ($\ell \geq 2$) MP amplitudes to Lorenz gauge. However, we note that while RW gauge is not defined for $\ell < 2$, there is no such restriction on the gauge transformation. Indeed, the work presented here can be directly extended to handle the transformations of nonradiative mode solutions from other gauges to Lorenz.

Throughout this paper we use the sign conventions and notation of Misner *et al.* [27] and use units in which $c = G = 1$. The background geometry is a nonrotating black hole which is described in terms of Schwarzschild coordinates $x^\mu = (t, r, \theta, \varphi)$.

II. FORMALISM

Consider the motion of a small compact object of mass μ in orbit about a static black hole of mass M, with $\mu/M \ll 1$. The small body gives rise to a perturbation

$p_{\mu\nu}$ in the metric relative to the Schwarzschild background,

$$ds^2 = g_{\mu\nu}dx^\mu dx^\nu = -f(r)dt^2 + f(r)^{-1}dr^2 + r^2(d\theta^2 + \sin^2\theta d\varphi^2), \tag{2.1}$$

where $f(r) = 1 - 2M/r$. We are concerned here only with the first-order part $p^{(1)}_{\mu\nu}$ of the MP in an expansion in powers of μ/M and accordingly simply set $p_{\mu\nu} = p^{(1)}_{\mu\nu}$. The full nonstationary metric is then $g_{\mu\nu} = g_{\mu\nu} + p_{\mu\nu}(t, r, \theta, \varphi)$. It often proves convenient to work with the trace-reversed MP

$$\bar{p}_{\mu\nu} = p_{\mu\nu} - \frac{1}{2}g_{\mu\nu}p_{\alpha\beta}g^{\alpha\beta}. \tag{2.2}$$

The Einstein field equations can be expanded about the background geometry. Once the stress-energy tensor $T^{(0)}_{\alpha\beta}$ associated with the motion of the small compact object has been specified, the first-order linear equations

$$G^{(1)}_{\alpha\beta}(\bar{p}_{\mu\nu}) = 8\pi T^{(0)}_{\alpha\beta} \tag{2.3}$$

can be solved to determine $\bar{p}_{\mu\nu}$. The small body is approximated as a point particle and the stress tensor is that of the particle moving on a geodesic of the Schwarzschild black hole (i.e., zeroth-order approximation).

In this work, we are interested in bound eccentric motion. The orbit is parametrized by a pair of constants, which can alternately be taken to be Darwin's [28] eccentricity e and dimensionless semilatus rectum p, or the bounding values of radial motion $r_{\rm min}$ and $r_{\rm max}$, or the specific energy $\mathcal{E}$ and angular momentum $\mathcal{L}$. The first integrals of motion are integrated using Darwin's curve parameter χ and are converted to functions of the form $r = r_p(t)$, $\varphi = \varphi_p(t)$, and $\tau = \tau_p(t)$ (with $\theta = \pi/2$). The orbit has two fundamental frequencies with a rate Ω_r associated with radial libration and a mean rate of azimuthal advance Ω_φ. See Darwin [28] for the orbital integration and Cutler *et al.* [29] for first application to black hole perturbations from bound motion.

A. Harmonic decomposition of the field equations

The usual route to solving the field equation (2.3) on a Schwarzschild background is to introduce tensor spherical harmonics and decompose the equations into individual angular harmonic modes. This approach was followed by Regge and Wheeler [30] and Zerilli [25] in solving for certain master functions that represent the odd- and even-parity parts, respectively, of the gravitational field. The MP is then derived from these master functions in Regge-Wheeler gauge. In Ref. [22], we used a variant of this approach, with slightly different versions of the two master functions, and combined it with a new analytic/numerical method for finding convergent solutions near the location of the point particle.

In that paper we followed Martel and Poisson [31] in using their definitions of the tensor spherical harmonics. We recap those definitions here. The unit two-sphere $\mathcal{S}^2$ is covered by coordinates (θ, φ). Upper-case latin indices A, B, etc. denote these two angular coordinates and associated tensor components. The coordinates (t, r) cover the submanifold $\mathcal{M}^2$. For these coordinates and tensor components, we use lowercase latin indices a, b, etc. The full Schwarzschild spacetime is $\mathcal{M} = \mathcal{M}^2 \times \mathcal{S}^2$. The usual scalar spherical harmonic functions are $Y^{\ell m}(\theta, \varphi)$. From these we define even-parity $Y^{\ell m}_A = D_A Y^{\ell m}$ and odd-parity $X^{\ell m}_A = -\varepsilon_A{}^B D_B Y^{\ell m}$ vector harmonics, where D_A is the covariant derivative on $\mathcal{S}^2$. The metric on the unit sphere is $\Omega_{AB} = \mathrm{diag}[1, \sin^2\theta]$ and the Levi-Civita tensor is ε_{AB}. Both are compatible with D_A: $D_C\Omega_{AB} = D_C\varepsilon_{AB} = 0$. Martel and Poisson define the two even-parity tensor spherical harmonics as $\Omega_{AB}Y^{\ell m}$ and $Y^{\ell m}_{AB} = [D_A D_B + \frac{1}{2}\ell(\ell+1)]Y^{\ell m}$, where the latter is trace free and thus differs from that used by Regge and Wheeler ($D_A D_B Y^{\ell m}$) [30]. They take the odd-parity tensor harmonic to be $X^{\ell m}_{AB} = -\frac{1}{2}(\varepsilon_A{}^C D_B + \varepsilon_B{}^C D_A)D_C Y^{\ell m}$, which differs by a minus sign from that of Regge and Wheeler [30].

Using these definitions, the MP is split into even- and odd-parity parts. Each parity is decomposed into sums over ℓ and m of their respective harmonics. For even parity there are seven amplitudes that Martel and Poisson define, which can be related to those of [25,30]. They are $h_{tt} = fH_0$, $h_{tr} = H_1$, $h_{rr} = H_2/f$, $j_t = h_0$, $j_r = h_1$, $G_{\rm here} = G_{\rm RW}$, and $K_{\rm here} = K_{\rm RW} - \ell(\ell+1)G/2$. (Note: here and on many occasions later in the text we suppress the spherical harmonic scripts ℓ and m for brevity when no confusion should arise.) Then the even-parity MP is

$$p_{ab} = \sum_{\ell,m} h^{\ell m}_{ab} Y^{\ell m}, \qquad p_{aB} = \sum_{\ell,m} j^{\ell m}_a Y^{\ell m}_B,$$
$$p_{AB} = r^2 \sum_{\ell,m} (K^{\ell m}\Omega_{AB}Y^{\ell m} + G^{\ell m}Y^{\ell m}_{AB}). \tag{2.4}$$

For odd parity there are three amplitudes, $h_t = h_0$, $h_r = h_1$, and $h^{\rm here}_2 = -h^{\rm RW}_2$, which are equivalent to the original definitions up to sign. The odd-parity MP is then

$$p_{aB} = \sum_{\ell,m} h^{\ell m}_a X^{\ell m}_B, \qquad p_{AB} = \sum_{\ell,m} h^{\ell m}_2 X^{\ell m}_{AB}, \tag{2.5}$$

along with the fact that $p_{ab} = 0$. For the balance of this paper we are only concerned with odd parity.

Regge-Wheeler gauge places the (algebraic) condition on the metric that $h^{\rm RW}_2 = 0$. In this gauge the odd-parity field equations become

$$
\begin{aligned}
-\partial_t\partial_r h_r^{\mathrm{RW}} + \partial_r^2 h_t^{\mathrm{RW}} - \frac{2}{r}\partial_t h_r^{\mathrm{RW}} - \frac{\ell(\ell+1)r-4M}{r^3 f} h_t^{\mathrm{RW}} &= P^t,\\
\partial_t^2 h_r^{\mathrm{RW}} - \partial_t\partial_r h_t^{\mathrm{RW}} + \frac{2}{r}\partial_t h_t^{\mathrm{RW}} + \frac{(\ell+2)(\ell-1)f}{r^2} h_r^{\mathrm{RW}} &= P^r,\\
-\frac{1}{f}\partial_t h_t^{\mathrm{RW}} + f\partial_r h_r^{\mathrm{RW}} + \frac{2M}{r^2} h_r^{\mathrm{RW}} &= P,
\end{aligned}
\tag{2.6}
$$

where the source amplitudes P^t, P^r, and P (for each ℓ and m) are odd-parity projections of the stress tensor,

$$
\begin{aligned}
P^a(t,r) &\equiv \frac{16\pi r^2}{\ell(\ell+1)} \int T^{aB} X_B^* d\Omega,\\
P(t,r) &\equiv 16\pi r^4 \frac{(\ell-2)!}{(\ell+2)!} \int T^{AB} X_{AB}^* d\Omega.
\end{aligned}
\tag{2.7}
$$

We use an asterisk to denote complex conjugation. The source amplitudes in turn satisfy the contracted Bianchi identity

$$
\frac{\partial P^t}{\partial t} + \frac{\partial P^r}{\partial r} + \frac{2}{r}P^r - \frac{(\ell-1)(\ell+2)}{r^2}P = 0, \tag{2.8}
$$

and the stress tensor itself is taken to be that of a particle in geodesic motion on the background geometry.

While in principle the coupled equations (2.6) might be solved to yield the metric in RW gauge, the usual approach involves defining and using one of several odd-parity master functions and solving a lone wave equation (master equation) for this function. The odd-parity part of the metric then is derived from the master function. An equivalent master function representation is used for even-parity in RW gauge. In our previous paper [22] we used the odd-parity Cunningham-Price-Moncrief (CPM) function [32], which we refer to here as Ψ_o. This gauge-invariant master function is defined in Regge-Wheeler gauge by

$$
\Psi_o(t,r) \equiv \frac{2r}{(\ell-1)(\ell+2)}\left[\partial_r h_t^{\mathrm{RW}} - \partial_t h_r^{\mathrm{RW}} - \frac{2}{r}h_t^{\mathrm{RW}}\right]. \tag{2.9}
$$

In terms of the tortoise coordinate $r_* = r + 2M\ln(r/2M-1)$, Ψ_o satisfies the wave equation

$$
\mathcal{W}_2\Psi_o(t,r) = S_o, \tag{2.10}
$$

where $\mathcal{W}_2$ is the spin-2 Regge-Wheeler operator, a particular case of the spin-s operator

$$
\mathcal{W}_s = -\frac{\partial^2}{\partial t^2} + \frac{\partial^2}{\partial r_*^2} - f\left[\frac{\ell(\ell+1)}{r^2} + \frac{2M(1-s^2)}{r^3}\right]. \tag{2.11}
$$

Later, we will have need for the Fourier transform of this operator ($\partial_t \to -i\omega$), which we will denote $\mathcal{L}_s$. The source term for the master equation involves a combination of moments of the stress tensor,

$$
\begin{aligned}
S_o(t,r) &\equiv \frac{2rf}{(\ell-1)(\ell+2)}\left[\frac{1}{f}\partial_t P^r + f\partial_r P^t + \frac{2M}{r^2}P^t\right]\\
&= \tilde{G}_o(t)\delta[r-r_p(t)] + \tilde{F}_o(t)\delta'[r-r_p(t)],
\end{aligned}
\tag{2.12}
$$

and is a distribution (see Ref. [22] for details). Once the CPM master function is known, the MP amplitudes in RW gauge can be reconstructed via the expressions

$$
\begin{aligned}
h_t^{\mathrm{RW}}(t,r) &= \frac{f}{2}\partial_r(r\Psi_o) - \frac{r^2 f}{(\ell-1)(\ell+2)}P^t,\\
h_r^{\mathrm{RW}}(t,r) &= \frac{r}{2f}\partial_t\Psi_o + \frac{r^2}{(\ell-1)(\ell+2)f}P^r.
\end{aligned}
\tag{2.13}
$$

Their numerical determination in the time domain with a convergent and accurate behavior everywhere including the vicinity of the moving particle was the subject of our previous paper.

Because we have reason to consider it in what follows, it is worthwhile noting that the original master function of Regge and Wheeler, Ψ_{RW}, is not the CPM master function we use. They are related by

$$
\Psi_{\mathrm{RW}}(t,r) = \frac{f}{r}h_r^{\mathrm{RW}}(t,r) = \frac{1}{2}\partial_t\Psi_o + \frac{r}{(\ell-1)(\ell+2)}P^r. \tag{2.14}
$$

The RW master function satisfies an almost identical wave equation,

$$
\mathcal{W}_2\Psi_{\mathrm{RW}}(t,r) = S_{\mathrm{RW}}, \tag{2.15}
$$

with the only difference being the source term

$$
S_{\mathrm{RW}}(t,r) \equiv \frac{f}{r}\left[-P^r + f\partial_r P - \frac{2}{r}\left(1-\frac{3M}{r}\right)P\right]. \tag{2.16}
$$

B. Gauge transformations

The exact form of the field equation (2.3) will depend upon specifying a gauge. As mentioned in the Introduction, two frequent choices are RW gauge and Lorenz (L) gauge. The small gauge generator Ξ^μ that transforms the coordinates $x^\mu_{\mathrm{L}} = x^\mu_{\mathrm{RW}} + \Xi^\mu$ between the two gauges is on the same order of magnitude as the MP, that is $|\Xi_\mu| \sim |\bar{p}_{\mu\nu}| \ll 1$. The MP then transforms as

$$
\bar{p}^{\mathrm{L}}_{\mu\nu} = \bar{p}^{\mathrm{RW}}_{\mu\nu} - \Xi_{\mu|\nu} - \Xi_{\nu|\mu} + g_{\mu\nu}\Xi^\alpha{}_{|\alpha}, \tag{2.17}
$$

where stroke $|\mu$ indicates covariant differentiation with respect to the background metric. Lorenz gauge requires the following condition on the MP,

$$
\bar{p}^{\mathrm{L}}_{\mu\nu}{}^{|\nu} = 0. \tag{2.18}
$$

Using this condition in Eq. (2.17) then provides a wave equation that must be satisfied by the gauge generator,

$$
\Xi_{\mu|\nu}{}^{\nu} = \bar{p}^{\mathrm{RW}|\nu}_{\mu\nu}. \tag{2.19}
$$

A gauge generator that satisfies this equation is unique only up to some Ξ'_μ that satisfies the homogeneous version of (2.19). Specifying the initial data and boundary values (if any) removes the residual gauge freedom and fully determines the gauge.

We consider next the spherical harmonic decomposition of the gauge vector. Momentarily considering again both even and odd parity, Ξ_μ can be broken down into

$$\Xi_a = \sum_{\ell,m}[\delta_a{}^t \xi_t^{\ell m}(t,r) + \delta_a{}^r \xi_r^{\ell m}(t,r)]Y_{\ell m},$$
$$\Xi_A = \sum_{\ell,m}[\xi_e^{\ell m}(t,r)Y_A^{\ell m} + \xi_o^{\ell m}(t,r)X_A^{\ell m}]. \tag{2.20}$$

There are three even-parity amplitudes and one odd-parity amplitude. We will concern ourselves with determining ξ_t, ξ_r, and ξ_e in a subsequent paper. In this paper we seek to obtain ξ_o. Substituting the decomposition of Ξ_μ into Eq. (2.19), we find after a bit of calculation that ξ_o satisfies the differential equation

$$\mathcal{W}_1 \xi_o(t,r) = 2f\Psi_{\rm RW} + fP. \tag{2.21}$$

Once the gauge generator amplitude is known, we decompose Eq. (2.17) in harmonic amplitudes and see that the odd-parity MP amplitudes are transformed by

$$h_t^{\rm L}(t,r) = h_t^{\rm RW} - \frac{\partial \xi_o}{\partial t},$$
$$h_r^{\rm L}(t,r) = h_r^{\rm RW} - \frac{\partial \xi_o}{\partial r} + \frac{2}{r}\xi_o, \tag{2.22}$$
$$h_2^{\rm L}(t,r) = -2\xi_o.$$

C. Local nature of the metric perturbation and gauge generator at $r = r_p(t)$

The rhs of Eq. (2.21) is singular at the location of the particle. In this sense Eq. (2.21) is very similar to Eq. (2.10). In Ref. [22] we examined Eq. (2.10) to determine the local behavior of Ψ_o. Assuming $\Psi_o = \Psi_o^+\theta[r - r_p(t)] + \Psi_o^-\theta[r_p(t) - r]$, we calculated jumps in the field, $[\![\Psi_o]\!]_p$, and in its radial derivative, $[\![\partial_r\Psi_o]\!]_p$. We use a subscript p to indicate that a function of r is evaluated at the location of the particle, $r = r_p(t)$, becoming a function of time.

Following the same logic here, we postulate a form for the gauge amplitude of $\xi_o = \xi_o^+\theta[r - r_p(t)] + \xi_o^-\theta[r_p(t) - r]$. Then, similar analysis to that found in Ref. [22], indicates that ξ_o is C^0, i.e., $[\![\xi_o]\!]_p = 0$. Further, we find the jump in the first radial derivative is

$$[\![\partial_r\xi_o]\!]_p(t) = \frac{f_p}{f_p^2 - \dot r_p^2}p. \tag{2.23}$$

Here $p(t)$ comes from the source amplitude P. All three source amplitudes are delta distributions with time-dependent amplitudes, $P = p(t)\delta[r - r_p(t)]$, $P^t = p^t(t)\delta[r - r_p(t)]$, and $P^r = p^r(t)\delta[r - r_p(t)]$.

Having computed the expected jumps in ξ_o and its radial derivative, we can use Eq. (2.22) to find the jumps in the Lorenz gauge MP amplitudes. As with the fields Ψ_o and ξ_o, we expect each MP amplitude to consist of left and right side differentiable functions that are joined at the location of the particle by Heaviside functions. We calculated the jumps in $h_t^{\rm RW}$ and $h_r^{\rm RW}$ in Ref. [22]. The discontinuities in the RW gauge MP amplitudes are exactly canceled out by terms arising from the derivatives of ξ_o and all three Lorenz gauge amplitudes are C^0 as expected. The jumps in their first derivatives are also analytically computable (either by examining the jumps in the higher-order derivatives of ξ_o or more simply by directly analyzing the Lorenz gauge field equations). We find

$$[\![\partial_r h_t]\!]_p(t) = \frac{f_p^2}{f_p^2 - \dot r_p^2}p^t,$$
$$[\![\partial_r h_r]\!]_p(t) = -\frac{1}{f_p^2 - \dot r_p^2}p^r, \tag{2.24}$$
$$[\![\partial_r h_2]\!]_p(t) = -\frac{2f_p}{f_p^2 - \dot r_p^2}p.$$

We use these expressions later (see Fig. 9) as a powerful check that we have correctly solved the gauge transformation equations to high accuracy.

III. TWO EHS-LIKE METHODS FOR EQUATIONS WITH NONCOMPACT SOURCES

In Ref. [22] we solved Eq. (2.10) for a variety of eccentric orbits. We used a FD approach to find the Fourier harmonic modes of Ψ_o and transformed back to the TD using the EHS method. The EHS method was first applied to wave equations with delta function sources. It allows TD reconstruction of the spherical harmonic amplitudes with exponential convergence, circumventing the Gibbs phenomenon that otherwise arises from solving equations with discontinuous or singular sources. Our application of the method also demonstrated it could be applied to sources with a derivative of a delta function.

With only a change in spin parameter, Eq. (2.21) has a similar differential operator as Eq. (2.10). Where the two equations differ markedly is in their source terms. While the source in Eq. (2.10) is point-singular and compact, the source in Eq. (2.21) is both distributional and noncompact. We can use the linearity of the equation to split off the singular part and split the generator into two parts, $\xi_o = \xi_o^{\rm ext} + \xi_o^{\rm sing}$, that satisfy separate equations,

$$\mathcal{W}_1\xi_o^{\rm sing}(t,r) = f_p p(t)\delta[r - r_p(t)], \tag{3.1}$$

$$\mathcal{W}_1\xi_o^{\rm ext}(t,r) = 2f\Psi_{\rm RW}. \tag{3.2}$$

While the former equation can be solved using the EHS method, the latter's extended source term is more problematic. The extended source is both noncompact and has a

time-dependent discontinuity that moves periodically between $r_{\min}$ and $r_{\max}$ as the particle orbits. In this section we present two equivalent methods for solving Eq. (3.2) using FD methods, both of which provide exponential convergence upon returning to the TD.

As discussed earlier, an eccentric orbit on Schwarzschild provides two fundamental frequencies. When we Fourier transform Eq. (3.2), we have a twofold countably infinite frequency spectrum,

$$\omega \equiv \omega_{mn} = m\Omega_\varphi + n\Omega_r, \qquad m, n \in \mathbb{Z}. \tag{3.3}$$

The Fourier transform and standard TD reconstruction of $\xi^{\rm ext}_o(t, r)$ is then

$$\begin{aligned} \tilde{\xi}^{\rm ext}_o(r) &\equiv \frac{1}{T_r}\int_0^{T_r} dt \xi^{\rm ext}_o(t, r) e^{i\omega t}, \\ \xi^{\rm ext}_o(t, r) &= \sum_{n=-\infty}^{\infty} \tilde{\xi}^{\rm ext}_o(r) e^{-i\omega t}. \end{aligned} \tag{3.4}$$

Note that in addition to the already suppressed indices ℓ and m, FD quantities have a third implied index, n. Equivalent expressions are used for the Fourier transforms and series representations of the other fields that we consider below. Note that while we use the standard tilde˜notation with $\tilde{\xi}^{\rm ext}_o$ to indicate a FD quantity, for other quantities we try to maintain consistency with previous literature by changing the base symbol. For the TD function $\Psi_{\rm RW}$, we write $R_{\rm RW}$ in the FD. Similarly, for its TD source term $S_{\rm RW}$, we write $Z_{\rm RW}$ in the FD.

A. First approach: Partial annihilator method

Our first method for solving Eq. (3.2) is a generalization of the standard method of annihilators used for solving inhomogeneous differential equations. It hinges on finding an "annihilator," a differential operator that gives a vanishing result after acting on the source. Then, one can act with the annihilator on both sides of the differential equation. What results is a homogeneous differential equation of higher order. Our strategy for solving Eq. (3.2) is essentially the same, except that because the initial source is discontinuous the operator that we find does not completely annihilate the rhs but instead converts it to a distribution. Hence, we refer to the operator as a partial annihilator.

The rhs of Eq. (3.2) is well suited to the method of partial annihilators because the Regge-Wheeler variable satisfies its own wave equation with a point-singular source, (2.15). Therefore, upon dividing Eq. (3.2) by f, we can take $\mathcal{W}_2$ as the partial annihilator and act on both sides of the equation

$$\begin{aligned} f\mathcal{W}_2\left(\frac{1}{f}\mathcal{W}_1\xi(t, r)\right) &= 2fS_{\rm RW}(t, r_p(t)) \\ &= 2f(\tilde{G}_{\rm RW}(t)\delta[r - r_p(t)] \\ &\quad + \tilde{F}_{\rm RW}(t)\delta'[r - r_p(t)]). \end{aligned} \tag{3.5}$$

For simplicity here and in the remainder of this section we drop the $^{\rm ext}_o$ tags. We have multiplied back through by f to ensure that the leading-order derivatives have unit coefficients. This differential equation is now fourth order, but its source is point-singular. This allow us to solve it using the EHS method, generalized to fourth-order equations. The specific form of the source in Eq. (3.5) is given by Martel [33], though we assume that both $\tilde{G}_{\rm RW}$ and $\tilde{F}_{\rm RW}$ have been evaluated at $r = r_p(t)$.

We Fourier transform Eq. (3.5) to obtain the FD equation

$$f\mathcal{L}_2\left(\frac{1}{f}\mathcal{L}_1\tilde{\xi}(r)\right) = 2fZ_{\rm RW}(r). \tag{3.6}$$

The Fourier transform averages the point source motion in time and produces $Z_{\rm RW}(r)$ which has support only within the source libration region $r_{\min} < r < r_{\max}$.

There are four linearly independent homogeneous solutions to Eq. (3.6). Two of these are the solutions to the second-order equation $\mathcal{L}_1\tilde{\xi} = 0$ and we denote them by $\tilde{\xi}^{\pm}_{h2}$. One behaves asymptotically as an outgoing wave at infinity while the other is downgoing at the horizon,

$$\tilde{\xi}^{-}_{h2} \sim e^{-i\omega r_*}(r \to 2M), \qquad \tilde{\xi}^{+}_{h2} \sim e^{i\omega r_*}(r \to \infty). \tag{3.7}$$

The other two solutions only satisfy the full fourth-order equation $\mathcal{L}_2(f^{-1}\mathcal{L}_1\tilde{\xi}) = 0$. As such we give them the label $h4$ and asymptotic analysis shows that

$$\tilde{\xi}^{-}_{h4} \sim f(r)e^{-i\omega r_*}(r \to 2M), \qquad \tilde{\xi}^{+}_{h4} \sim re^{i\omega r_*}(r \to \infty). \tag{3.8}$$

These four solutions form a basis spanning the space of homogeneous solutions of Eq. (3.6). The particular solution will be a linear combination of these with variable coefficients,

$$\begin{aligned} \tilde{\xi}_p(r) = c^{-}_{h2}(r)\tilde{\xi}^{-}_{h2}(r) + c^{+}_{h2}(r)\tilde{\xi}^{+}_{h2}(r) + c^{-}_{h4}(r)\tilde{\xi}^{-}_{h4}(r) \\ + c^{+}_{h4}(r)\tilde{\xi}^{+}_{h4}(r). \end{aligned} \tag{3.9}$$

The four normalization functions $c^{\pm}_{h2/h4}(r)$ are fixed by the method of variation of parameters, which entails solving the equations

$$\frac{dc^{\pm}_{h2/h4}}{dr_*} = 2fZ_{\rm RW}(r)\frac{W^{\pm}_{h2/h4}(r)}{W(r)}. \tag{3.10}$$

Here $W(r)$ is the Wronskian and $W^{\pm}_{h2/h4}(r)$ is the "modified Wronskian" (Cramer's rule), which is the Wronskian with the column corresponding to the $\xi^{\pm}_{h2/h4}(r)$ homogeneous solution replaced by the column vector (0, 0, 0, 1). Note that because the differential operator in Eq. (3.5) is written in terms of r_*, the derivatives within the Wronskian must also be taken with respect to r_* and the lhs of Eq. (3.10) is a derivative taken with respect to r_*. For the two "+" equations, the integral form of Eq. (3.10) is (we change the variable of integration to r and see the factor of f cancel)

$$c^{+}_{h2/h4}(r) = 2\int_{r_{\rm min}}^{r}\left[\frac{1}{T_r}\int_0^{T_r}(\tilde{G}_{\rm RW}(t)\delta[r'-r_p(t)] + \tilde{F}_{\rm RW}(t)\delta'[r'-r_p(t)])e^{i\omega t}dt\right]\frac{W^{+}_{h2/h4}(r')}{W(r')}dr'. \tag{3.11}$$

Likewise, for the two "$-$" equations (note the change on the limits of integration),

$$c^{-}_{h2/h4}(r) = 2\int_{r}^{r_{\rm max}}\left[\frac{1}{T_r}\int_0^{T_r}(\tilde{G}_{\rm RW}(t)\delta[r'-r_p(t)] + \tilde{F}_{\rm RW}(t)\delta'[r'-r_p(t)])e^{i\omega t}dt\right]\frac{W^{-}_{h2/h4}(r')}{W(r')}dr'. \tag{3.12}$$

The EHS method requires knowing only the terminal values of the four functions $c^{\pm}_{h2/h4}(r)$, i.e., $C^{+}_{h2/h4} = c^{+}_{h2/h4}(r_{\rm max})$ and $C^{-}_{h2/h4} = c^{-}_{h2/h4}(r_{\rm min})$. Switching the order of integration and integrating by parts, we find

$$C^{\pm}_{h2/h4} = \frac{2}{T_r}\int_0^{T_r}\left\{\tilde{G}_{\rm RW}(t)\frac{W^{\pm}_{h2/h4}(r_p)}{W(r_p)} - \tilde{F}_{\rm RW}(t) \times\left[-\frac{W^{\pm}_{h2/h4}(r_p)}{W(r_p)^2}\partial_r W(r_p) + \frac{\partial_r W^{\pm}_{h2/h4}(r_p)}{W(r_p)}\right]\right\}e^{i\omega t}dt. \tag{3.13}$$

At this point we define the EHS in the FD to be

$$\begin{aligned}\tilde{\xi}^{-}_{h}(r) &\equiv C^{-}_{h2}\tilde{\xi}^{-}_{h2}(r) + C^{-}_{h4}\tilde{\xi}^{-}_{h4}(r),\\ \tilde{\xi}^{+}_{h}(r) &\equiv C^{+}_{h2}\tilde{\xi}^{+}_{h2}(r) + C^{+}_{h4}\tilde{\xi}^{+}_{h4}(r),\end{aligned} \tag{3.14}$$

and the EHS in the TD are defined by the Fourier sums (recall the suppressed ℓ, m, n indices)

$$\xi^{\pm}(t,r) \equiv \sum_n \tilde{\xi}^{\pm}_{h}(r)e^{-i\omega t}. \tag{3.15}$$

The extension of these solutions to $r = r_p(t)$ then gives the desired solution to Eq. (3.2),

$$\xi^{\rm ext}_{o}(t,r) = \xi^{+}(t,r)\theta[r-r_p(t)] + \xi^{-}(t,r)\theta[r_p(t)-r]. \tag{3.16}$$

B. Second approach: Method of extended particular solutions

Now we look for a solution to Eq. (3.2) that does not require a partial annihilator. In the FD the equation transforms to

$$\mathcal{L}_1\tilde{\xi}^{\rm ext}_{o}(r) = 2fR_{\rm RW}. \tag{3.17}$$

Again, for notational simplicity we drop the $^{\rm ext}_{o}$ tags for the remainder of this section. In the end we want solutions to Eq. (3.17) that allow us to form an exponentially converging solution to Eq. (3.2) when we transfer to the TD. This will require a new technique, which we call extended particluar solutions, and is closely analogous to the EHS method. First, though, we consider how to get the correct causal solution to Eq. (3.17) from a "standard" approach.

In the subsequent sections we make a distinction between quantities with ∞ and H tags which designate functions computed from a "standard" rhs source [Eq. (3.23) below] and those quantities with $+$ and $-$ tags which designate functions computed from an "extended" rhs source [Eq. (3.32) below]. Because the homogeneous solutions do not depend on the source, we always tag them with $+$ or $-$. We distinguish between particular and homogeneous solutions by using the respective subscripts p and h.

1. Finding standard FD solutions with causal boundary conditions

By examining the source, $2fR_{\rm RW}$, and the differential operator, $\mathcal{L}_1$, we can obtain asymptotic and Taylor expansions of the particular solution $\tilde{\xi}_p$ near infinity and the horizon, respectively. The expansions are useful numerically but for our purposes here we need only consider the leading asymptotic dependence. (See the Appendix for discussion of the asymptotic expansion ($r\to\infty$) of $\tilde{\xi}_p$ and how it couples to the expansion of $R_{\rm RW}$.)

Consider first the spatial infinity side. Let the RW function have an asymptotic amplitude $C^{+}_{\rm RW}$, so $R_{\rm RW} = C^{+}_{\rm RW}e^{i\omega r_*}$ as $r_*\to\infty$. We then make the ansatz that $\tilde{\xi}_p = C^{\infty}_{p}re^{i\omega r_*}$ as $r_*\to\infty$. Using an asymptotic approximation to Eq. (3.17) we find

$$\left(\frac{d^2}{dr_*^2}+\omega^2\right)(C^{\infty}_{p}re^{i\omega r_*}) = 2C^{+}_{\rm RW}e^{i\omega r_*} \Rightarrow C^{\infty}_{p} = \frac{1}{i\omega}C^{+}_{\rm RW}. \tag{3.18}$$

Therefore, the asymptotic form of $\tilde{\xi}^{\infty}_{p}$ is

$$\tilde{\xi}^{\infty}_{p} = -\frac{i}{\omega}C^{+}_{\rm RW}re^{i\omega r_*}, \qquad r\to\infty. \tag{3.19}$$

Next we consider the horizon side. The RW function is asymptotically $R_{\rm RW} = C^{-}_{\rm RW}e^{-i\omega r_*}$ as $r_*\to-\infty$. In this case we expect the particular solution to behave as $\tilde{\xi}_p = C^{H}_{p}fe^{-i\omega r_*}$ as $r_*\to-\infty$. Again, acting with the near-horizon leading parts of the differential operator, we find

$$\left(\frac{d^2}{dr_*^2}+\omega^2\right)(C^{H}_{p}fe^{-i\omega r_*}) = 2fC^{-}_{\rm RW}e^{-i\omega r_*} \Rightarrow C^{H}_{p} = 2\left(\frac{1}{4M^2}-\frac{i\omega}{M}\right)^{-1}C^{-}_{\rm RW}. \tag{3.20}$$

Therefore, the near-horizon form of $\tilde{\xi}^{H}_{p}$ is

$$\tilde{\xi}^{H}_{p} = 2\left(\frac{1}{4M^2}-\frac{i\omega}{M}\right)^{-1}C^{-}_{\rm RW}fe^{-i\omega r_*}, \qquad r\to 2M. \tag{3.21}$$

We can use Eqs. (3.19) and (3.21) to set boundary conditions (B.C.'s) for two separate integrations of the inhomogeneous differential equation (3.17) (yielding two different particular solutions that differ by some homogeneous solution). This integration requires the source $R_{\rm RW}$, which is itself the solution to the differential equation

$$\mathcal{L}_2 R_{\rm RW}(r) = Z_{\rm RW}(r). \tag{3.22}$$

We find it by variation of parameters, which yields

$$R^{\rm std}_{\rm RW}(r) = c^+_{\rm RW}(r)\hat{R}^+(r) + c^-_{\rm RW}(r)\hat{R}^-(r), \tag{3.23}$$

where $\hat{R}^\pm(r)$ are unit-normalized homogeneous solutions to Eq. (3.22). Note that $c^+_{\rm RW}(r \geq r_{\rm max}) = C^+_{\rm RW}$ and $c^-_{\rm RW}(r \leq r_{\rm min}) = C^-_{\rm RW}$. Furthermore, the solution $R^{\rm std}_{\rm RW}(r)$ is *not* the same as the EHS to Eq. (3.22).

Having solved Eq. (3.22) for the source term in Eq. (3.23) and determined the B.C.'s, we are ready to solve Eq. (3.17). The idea is to find the two different particular solutions, neither of which has the proper causal behavior, and then correct for the acausality by adding appropriate homogeneous solutions. The result of this process is a solution to Eq. (3.17) with causal behavior on both sides. The details follow in a series of steps.

(1) Solve for the particular solution from the spatial-infinity side (see Fig. 2).
We set a B.C. to Eq. (3.17) using Eq. (3.19) and integrate to large negative r_* using Eq. (3.23) as the source. Although the starting B.C. specified no homogeneous contribution, homogeneous solutions on the horizon side will be excited. See the left side of Fig. 2. The particular solution integrated from the spatial infinity side has the asymptotic behavior,

$$\tilde{\xi}^\infty_p = \begin{cases} C^\infty_p r e^{i\omega r_*}, & r_* \to +\infty, \\ C^H_p f e^{-i\omega r_*} + \kappa^+ e^{i\omega r_*} + \kappa^- e^{-i\omega r_*}, & r_* \to -\infty. \end{cases} \tag{3.24}$$

The term with coefficient C^H_p is the part directly dependent on the source and it is subdominant in comparison to the homogeneous solutions. The coefficients $\kappa^\pm$ are to be determined. Importantly, $\kappa^+ e^{i\omega r_*}$ is an acausal term (upgoing from the past horizon).

(2) Solve for the particular solution from the horizon side (see Fig. 3).
We set a B.C. to Eq. (3.17) using Eq. (3.21) and integrate to large positive r_* using Eq. (3.23) as the source. Although the starting B.C. specified no homogeneous contribution, homogeneous solutions on the spatial infinity side will be excited. The effect can be seen on the right side of Fig. 3. The particular solution dominates, but the constant offset between real and imaginary parts indicates the presence of asymptotically constant-amplitude homogeneous terms. Analysis shows that the particular solution integrated from the horizon will behave as

$$\tilde{\xi}^H_p = \begin{cases} C^H_p f e^{-i\omega r_*}, & r_* \to -\infty, \\ C^\infty_p r e^{i\omega r_*} + \lambda^- e^{-i\omega r_*} + \lambda^+ e^{i\omega r_*}, & r_* \to +\infty. \end{cases} \tag{3.25}$$

The coefficients $\lambda^\pm$ are to be determined, and again we find an acausal term ($\lambda^- e^{-i\omega r_*}$), which in this case is ingoing from past null infinity.

(3) Solve for the homogeneous solution from the spatial infinity side.
Next, we set an outgoing B.C. to the homogeneous version of Eq. (3.17) at large positive r_*. We integrate to solve the scattering problem for reflection and transmission amplitudes R^+ and T^+ [34]. In the terminology of Gal'tsov [35], this is an "up" mode,

$$\tilde{\xi}^+_h = \begin{cases} T^+ e^{i\omega r_*}, & r_* \to +\infty, \\ R^+ e^{-i\omega r_*} + e^{i\omega r_*}, & r_* \to -\infty. \end{cases} \tag{3.26}$$

Scaled appropriately, this solution can be added to Eq. (3.24) to remove its acausality.

(4) Solve for the homogeneous solution from the horizon side.

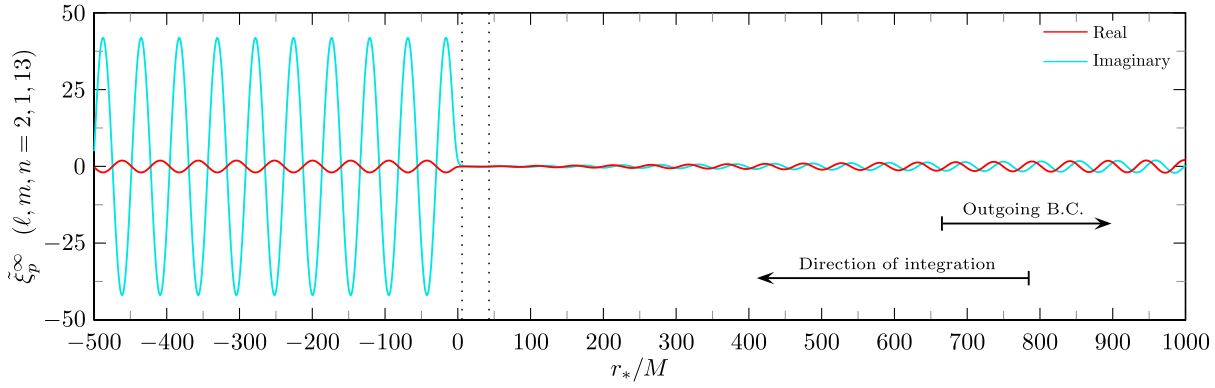

FIG. 2 (color online). Integration from large r_* of the particular solution, $\tilde{\xi}^\infty_p$. Dotted lines indicate the source libration region.

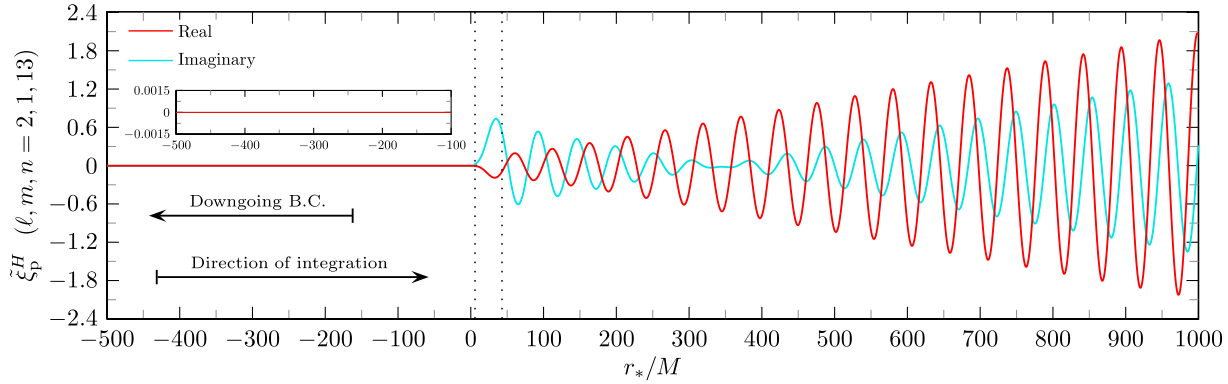

FIG. 3 (color online). Integration from large negative r_* of the particular solution, $\tilde{\xi}^H_p$. Dotted lines indicate the source libration region.

We set a downgoing B.C. to the homogeneous version of Eq. (3.17) at large negative r_* and integrate to solve the scattering problem for reflection and transmission amplitudes R^- and T^-. This is an "in" mode,

$$\tilde{\xi}^-_h = \begin{cases} T^- e^{-i\omega r_*}, & r_* \to -\infty, \\ R^- e^{i\omega r_*} + e^{-i\omega r_*}, & r_* \to +\infty. \end{cases} \tag{3.27}$$

Scaled appropriately, this solution can be added to Eq. (3.25) to remove its acausality.

(5) Resolve the acausality in the particular solutions (see Fig. 4).

The acausal piece in Eq. (3.24) is $\kappa^+ e^{i\omega r_*}$. Using Eq. (3.26), we can remove this by subtracting $\kappa^+ \tilde{\xi}^+_h$,

$$\tilde{\xi}^\infty_p - \kappa^+ \tilde{\xi}^+_h = \begin{cases} C^\infty_p r e^{i\omega r_*} - \kappa^+ T^+ e^{i\omega r_*}, & r_* \to +\infty, \\ C^H_p f e^{-i\omega r_*} + \kappa^- e^{-i\omega r_*} - \kappa^+ R^+ e^{-i\omega r_*}, & r_* \to -\infty. \end{cases} \tag{3.28}$$

The acausal piece in Eq. (3.25) is $\lambda^- e^{-i\omega r_*}$. Using Eq. (3.27), we can remove this by subtracting $\lambda^- \tilde{\xi}^-_h$,

$$\tilde{\xi}^H_p - \lambda^- \tilde{\xi}^-_h = \begin{cases} C^H_p f e^{-i\omega r_*} - \lambda^- T^- e^{-i\omega r_*}, & r_* \to -\infty, \\ C^\infty_p r e^{i\omega r_*} + \lambda^+ e^{i\omega r_*} - \lambda^- R^- e^{i\omega r_*}, & r_* \to +\infty. \end{cases} \tag{3.29}$$

Equations (3.28) and (3.29) are both solutions to Eq. (3.17) and both satisfy the causal nature of the problem. Therefore they must be equal. In order to form them, we must know κ^+ and λ^-. We find them by setting Eqs. (3.28) and (3.29) and their first derivatives equal at any point,

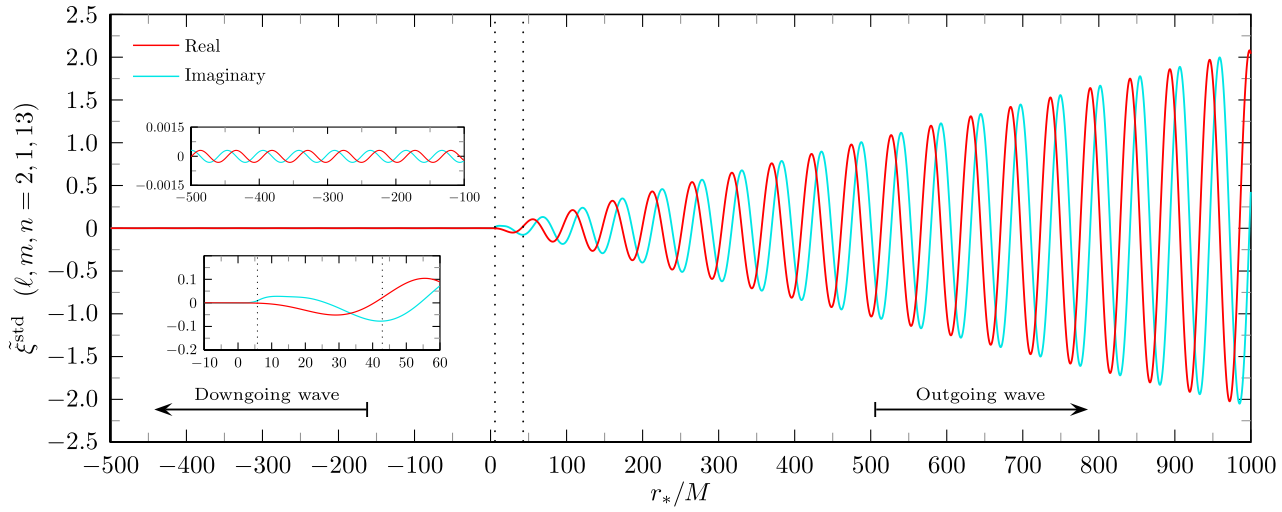

FIG. 4 (color online). Causally correct solution to Eq. (3.17), $\tilde{\xi}^{\rm std}$. Dotted lines indicate the source libration region.

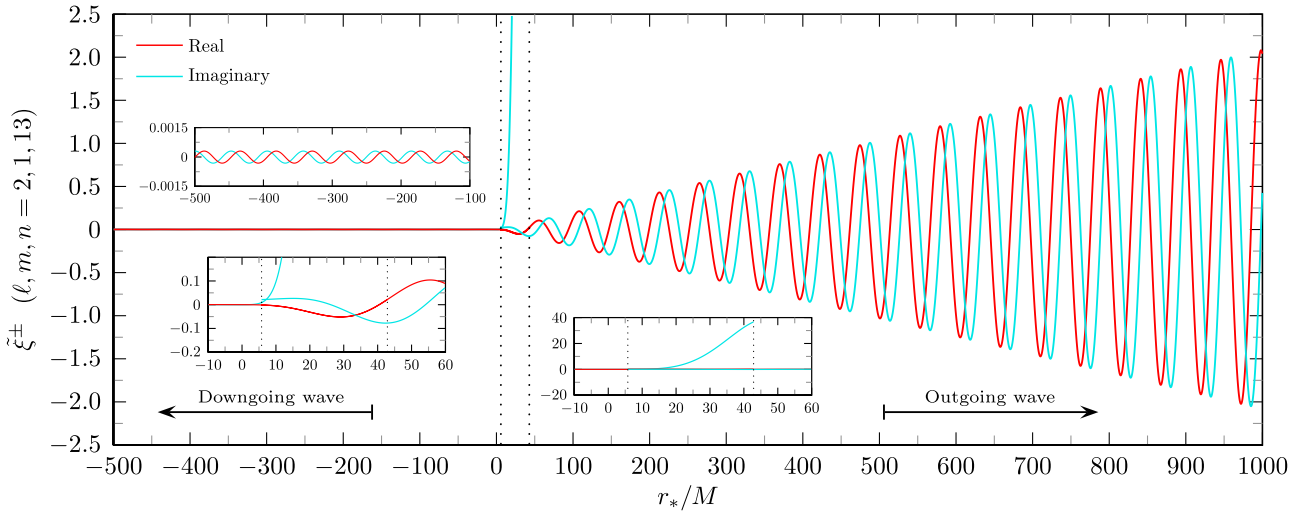

FIG. 5 (color online). Causally correct extended particular solution, $\tilde{\xi}^{\pm}$. Note the difference within the libration region (shown in dotted lines), between $\tilde{\xi}^{\pm}$ and $\tilde{\xi}^{\rm std}$ (Fig. 4). The difference in TD convergence between these two solutions is shown later in Fig. 8.

$$\tilde{\xi}^{H}_{p} - \lambda^{-}\tilde{\xi}^{-}_{h} = \tilde{\xi}^{\infty}_{p} - \kappa^{+}\tilde{\xi}^{+}_{h}, \tag{3.30}$$

$$\partial_{r_*}\tilde{\xi}^{H}_{p} - \lambda^{-}\partial_{r_*}\tilde{\xi}^{-}_{h} = \partial_{r_*}\tilde{\xi}^{\infty}_{p} - \kappa^{+}\partial_{r_*}\tilde{\xi}^{+}_{h}. \tag{3.31}$$

We solve these equations for κ^{+} and λ^{-} and form $\tilde{\xi}^{H}_{p} - \lambda^{-}\tilde{\xi}^{-}_{h}$ and $\tilde{\xi}^{\infty}_{p} - \kappa^{+}\tilde{\xi}^{+}_{h}$, which are equivalent. In principle, one could pick any point and expect the same result. In practice, slight numerical differences occur. In fact, we use several points to determine these constants and use the discrepancies that are found as a measure of the order of magnitude of the error. Cumulative numerical error in the solutions is addressed in Sec. IV.

The function $\tilde{\xi}^{\rm std}_{p} = \tilde{\xi}^{H}_{p} - \lambda^{-}\tilde{\xi}^{-}_{h} = \tilde{\xi}^{\infty}_{p} - \kappa^{+}\tilde{\xi}^{+}_{h}$ represents the standard solution to Eq. (3.17). If the TD source were differentiable, we would be able to find the corresponding TD solution via an exponentially converging Fourier synthesis. However, the source in this case is nondifferentiable, and we need an EHS-like trick to complete the method.

2. Restoring exponential convergence with extended particular solutions

The EHS of the Regge-Wheeler equation, Eq. (3.22), are found by taking the constants $C^{\pm}_{\rm RW}$ and scaling the unit-normalized homogeneous solutions,

$$R^{\pm}_{\rm RW}(r) \equiv C^{\pm}_{\rm RW}\hat{R}^{\pm}(r). \tag{3.32}$$

These solutions are defined for all $r > 2M$. In like fashion we seek to find FD EPS of Eq. (3.17) and denote these by $\tilde{\xi}^{\pm}$. We first find $\tilde{\xi}^{\pm}_{p}$ by separately integrating Eq. (3.17) with the modified source terms $R^{\pm}_{\rm RW}$. The solutions are each made to match the exterior behavior of $\tilde{\xi}^{\rm std}_{p}$ by adding the correctly scaled homogeneous solutions found in Step III B 1 above. We then define

$$\tilde{\xi}^{+} \equiv \tilde{\xi}^{+}_{p} - \kappa^{+}\tilde{\xi}^{+}_{h}, \qquad \tilde{\xi}^{-} \equiv \tilde{\xi}^{-}_{p} - \lambda^{-}\tilde{\xi}^{-}_{h}. \tag{3.33}$$

See Fig. 5, which contrasts Fig. 4 in the source region.

These FD EPS can be transferred to the TD via Fourier series,

$$\xi^{\pm}(t, r) \equiv \sum_{n}\tilde{\xi}^{\pm}(r)e^{-i\omega t}. \tag{3.34}$$

The solution to Eq. (3.2) is then the weak solution,

$$\xi^{\rm ext}_{o}(t, r) = \xi^{+}(t, r)\theta[r - r_p(t)] + \xi^{-}(t, r)\theta[r_p(t) - r]. \tag{3.35}$$

The support for this claim has three legs. Firstly, the same arguments about EHS, based on analytic continuation, made by Barack *et al.* in Ref. [19] appear to apply in extension to Eq. (3.2) as well. Secondly, we demonstrate existence numerically by integrating the equation, with causal boundary conditions, and checking that the jump conditions (internal boundary conditions) at the particle are satisfied. One then appeals to the linearity of the equation to establish uniqueness. Finally, we have an independent numerical solution found through the method of partial annihilators and given in Eq. (3.16). We have confirmed that the two methods give entirely consistent solutions. These results are covered in detail in the next section.

IV. RESULTS

The methods of the previous section allow us to transform odd-parity solutions of the first-order Einstein equations from RW to Lorenz gauge. As an example, we consider an orbit with eccentricity $e = 0.764124$ and semi-latus rectum $p = 8.75455$. This orbit was used in Fig. 1 where we showed the RW amplitudes h_t and h_r for $\ell = 2$ and $m = 1$ ($h_2 = 0$). The MPs can be evaluated at any time

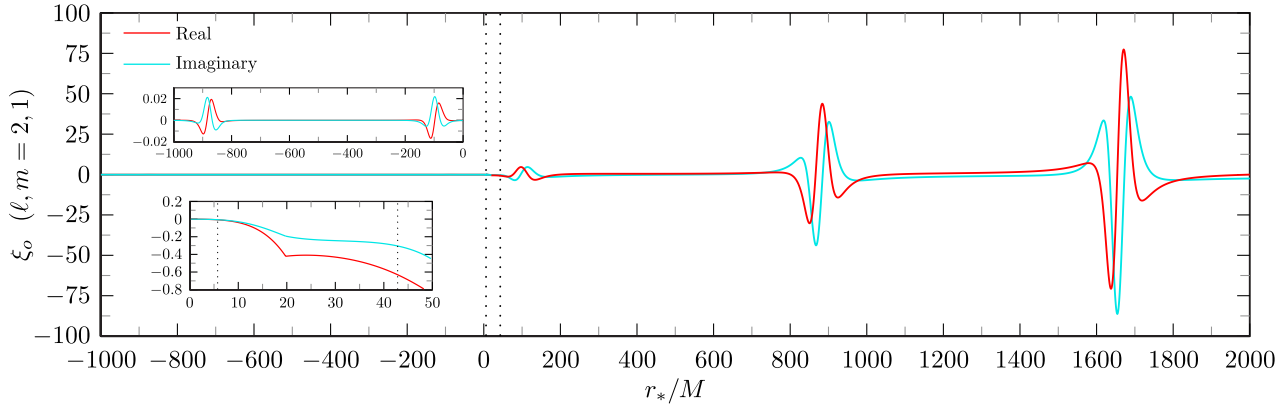

FIG. 6 (color online). The $\ell = 2, m = 1$ mode of the odd-parity RW-to-Lorenz gauge generator amplitude ξ_o. The Lorenz gauge MP amplitude h_2 differs from ξ_o only by a factor of -2. Dotted lines indicate the region of libration. Orbital parameters are given in the text. While the field h_2 grows asymptotically, upon transforming to an orthonormal frame, it would contribute a term that falls off as $1/r$.

but we chose to display results at $t = 93.58$ (where $t = 0$ is at the periapsis). The RW modes are discontinuous at $r = r_p(t)$ and lack asymptotic flatness. The gauge generator to go from RW to Lorenz gauge is computed for this same orbit and at the same time in the TD. It is used to obtain the MPs in Lorenz gauge using Eq. (2.22). Figure 6 shows the $\ell = 2, m = 1$ amplitude of the gauge generator itself, which differs from h_2 in Lorenz gauge only by a factor of -2. Figure 7 shows the Lorenz gauge metric amplitudes h_t^{L} and h_r^{L} for the same mode. The MPs are now C^0 at $r = r_p(t)$ and are asymptotically flat.

Of key importance to our method is the exponential convergence of the TD solutions. We can first consider self-convergence of the modes for all r. As an example we choose an orbit with $e = 0.188917$ and $p = 7.50478$ at time $t = 96.44$. In Fig. 8 we show the self-convergence of $\xi_o(r)$ for a set of partial Fourier sums over n from $-N \leq n \leq +N$ for various N. The right panel of this figure shows

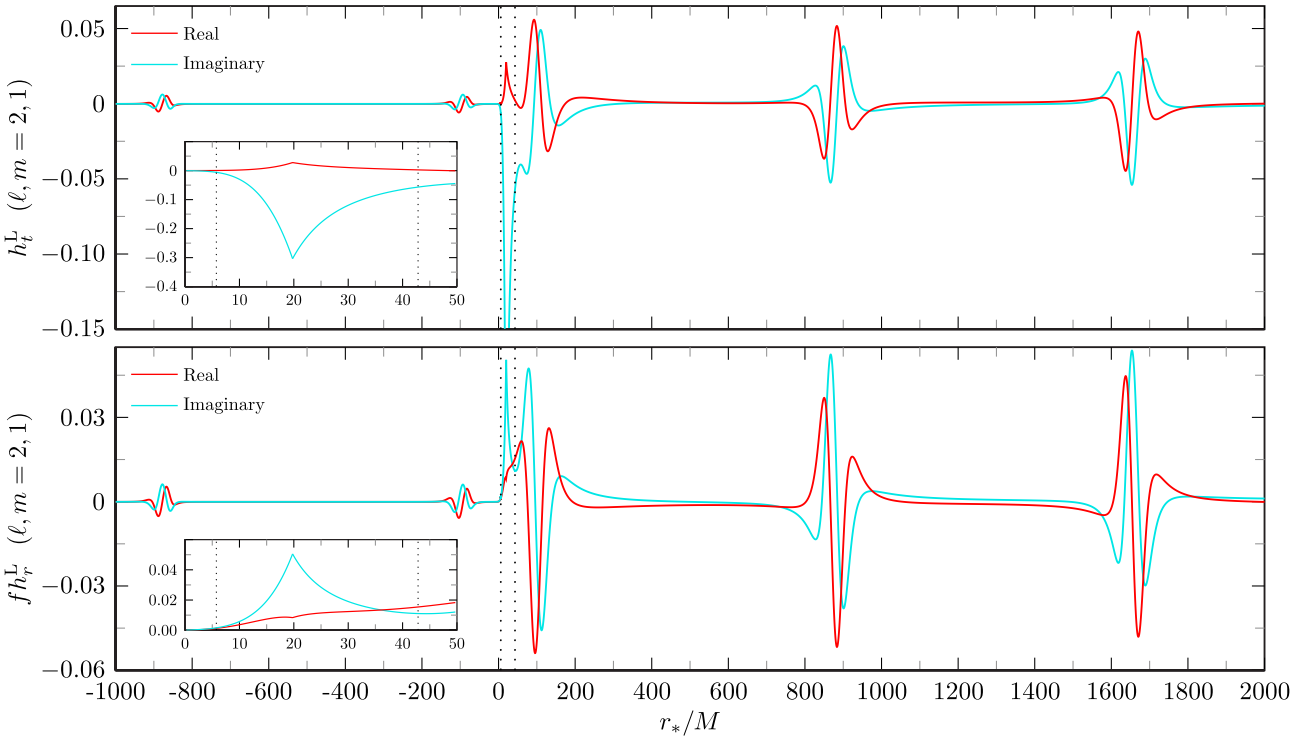

FIG. 7 (color online). The $\ell = 2, m = 1$ mode of the Lorenz gauge MP amplitudes h_t^{L} and h_r^{L}. Dotted lines indicate the region of libration. Orbital parameters are given in the text. Note (comparing to Fig. 1) the discontinuity at the location of the particle has vanished and the wave no longer grows asymptotically. We plot $f h_r^{\mathrm{L}}$ so we can see the wave behavior near the horizon.

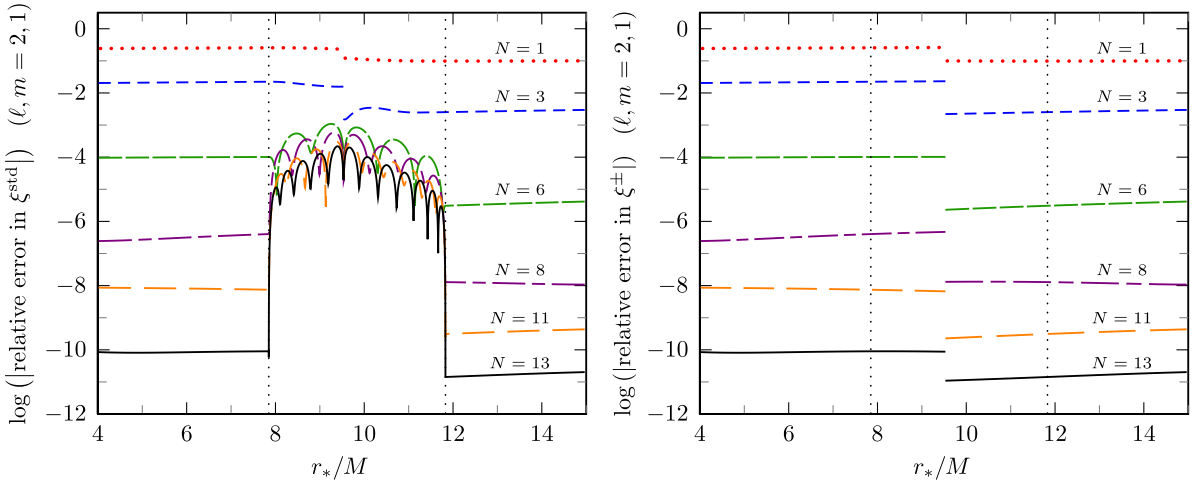

FIG. 8 (color online). Self-convergence of the $\ell = 2$, $m = 1$ mode of ξ_o. We show results for the standard method in the left panel and our (equivalent) partial annihilators and EPS on the right. The orbital parameters are $e = 0.188917$ and $p = 7.50478$, and the fields are calculated at time $t = 96.44$.

exponential self-convergence of the EPS method as a function of r, including at the particle. This result is in contrast with the left panel which shows that the standard method is only algebraically convergent in the source libration region. Note that the convergence is initially exponential before becoming algebraic around an error level of 10^{-4}. This transition is due to the equation for ξ_o having singular and extended parts [see Eqs. (3.1) and (3.2)]. We find the singular part using EHS, which converges exponentially. This part of the solution dominates the self-convergence in the left panel at first. Eventually, the lack of differentiability of the extended source and the use (for comparison) of the standard Fourier series for that part of the field manifests itself. The appearance of Gibbs behavior stalls the convergence in the libration region.

Beyond self-convergence, we can check absolute convergence to the analytically known jump conditions. This test can be applied to both the MP amplitudes and their first radial derivatives. As shown in the left panel of Fig. 9, we find exponential convergence to the analytically computed values in Eq. (2.24), in this case using the partial annihilator method. Here the orbit is the more eccentric one with $e = 0.764124$ and $p = 8.75455$. Each partial Fourier sum ranges over all harmonics from $-N \le n \le +N$ for different values of N as seen on the horizontal axis. The jump conditions are time dependent and thus we compare our results at several moments in time (in this case at 20 points)

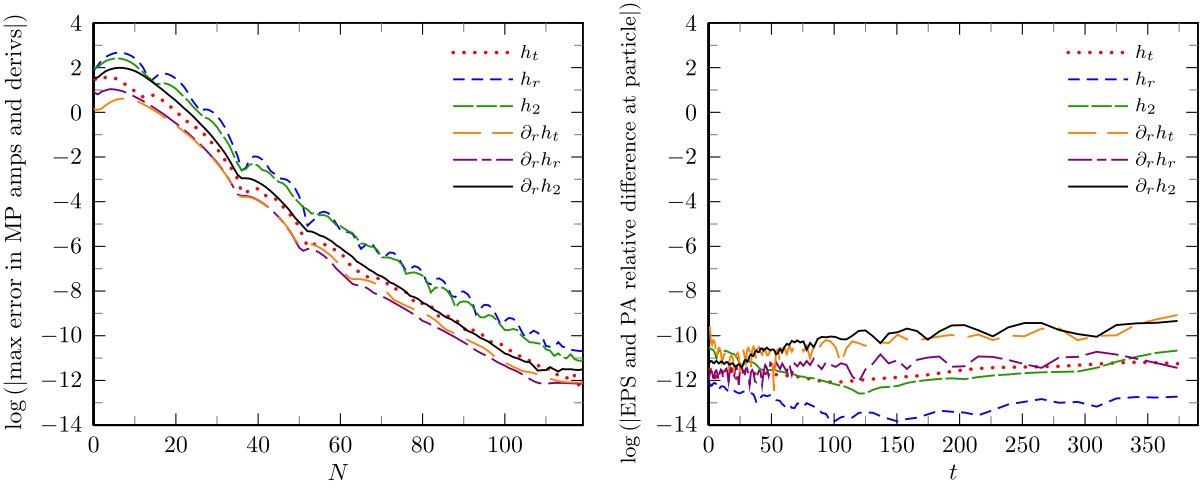

FIG. 9 (color online). Convergence of the jump conditions as a measure of solution error. In the left panel the partial annihilator method was used to compute the gauge generator and MPs for a high eccentricity orbit with $e = 0.764124$ and $p = 8.75455$. Partial Fourier sums over n are computed with $-N \le n \le +N$ and for various N. Exponential convergence is exhibited in the various sums. See text for further discussion. In the right panel a comparison is made of discrepancies between the EPS method and the PA method as a function of time about the orbit. See further discussion in the text.

throughout the orbit. The left panel plots the maximum error encountered in each quantity throughout an orbit. Since the Lorenz gauge amplitudes are all C^0, we plot absolute convergence for the jumps in the amplitudes themselves (which are expected to converge to 0) and relative convergence for the jumps in the r derivatives of the amplitudes. The convergence appears to bottom out around 10^{-12} to 10^{-11}.

In the right panel of Fig. 9, we compare the accuracy of the EPS and PA methods. For the jumps in Lorenz gauge MP amplitudes and their radial derivatives, we show the relative error between the two methods as a function of time throughout one orbit. The same high eccentricity orbit is used, though to compare the two methods the partial Fourier sums were fixed and taken to range over $-85 \leq n \leq 106$. The two methods agree with each other to the level of 10^{-12} to 10^{-10}.

Although we have only displayed results in this paper for the $\ell = 2$, $m = 1$ mode, we have run the code on many different modes and for different orbits. We have no difficulty in computing the gauge transformation from RW to Lorenz for odd-parity modes with high accuracy. It now remains for us to apply these methods to the even-parity part of the gauge transformation, a somewhat more involved procedure. We will turn to that issue in a subsequent paper.

V. CONCLUSION

This paper is the first of two on the transformation of metric perturbations from Regge-Wheeler gauge to Lorenz gauge. This first paper was confined to treating the odd-parity part of the MPs and devoted much of the discussion to the development of two new analytic/numerical methods for using frequency domain methods to find accurate solutions in the time domain. The follow-on paper will be primarily devoted to discussing the analytic problem of finding the even-parity part of the gauge transformation and will draw upon the numerical methods which we have detailed here.

ACKNOWLEDGMENTS

The authors thank Chad Galley and Ian Hinder for helpful discussions. We also appreciate suggestions made by the referee. C. R. E. acknowledges support from the Bahnson Fund at the University of North Carolina-Chapel Hill.

APPENDIX: ASYMPTOTIC EXPANSIONS AND BOUNDARY CONDITIONS

In the RWZ formalism it is useful to compute asymptotic expansions of the master functions about $r = \infty$ to provide boundary conditions for starting numerical integrations at finite radius. In this paper, the inhomogeneous equation for the gauge generator, Eq. (3.17), has a source term that is noncompact. This fact leads to an inhomogeneous recurrence relation for the asymptotic expansion of $\tilde{\xi}_o$ that requires as input the asymptotic expansion of the source term.

We start by writing

$$\tilde{\xi}_o = rJ_o(r)e^{i\omega r_*}, \tag{A1}$$

where $J_o(r)$ is the Jost function [34], which goes to 1 at infinity. We use Eq. (2.14) to express the rhs of Eq. (3.17) in terms of the CPM function. Then we Fourier transform that function and plug in Eq. (A1) to obtain

$$rf\frac{d^2}{dr^2}J_o + 2\left(1 + i\omega r - \frac{M}{r}\right)\frac{d}{dr}J_o + \left(2i\omega + \frac{2M}{r^2} - \frac{\ell(\ell+1)}{r}\right)J_o = -i\omega J_R. \tag{A2}$$

Here $J_R = J^+_{\ell mn}$ from Appendix D of Ref. [22]. Now, we assume the following forms of J_o and J_R,

$$J_o(r) = \sum_{j=0}^{\infty}\frac{a^o_j}{(r\omega)^j}, \qquad J_R(r) = \sum_{j=0}^{\infty}\frac{a^R_j}{(r\omega)^j}. \tag{A3}$$

Plugging these in and assuming the equation is satisfied order-by-order gives the coupled recurrence formula,

$$2i(j-1)a^o_j = [(j-2)(j-1) - \ell(\ell+1)]a^o_{j-1} + 2M\omega[1-(j-2)^2]a^o_{j-2} + ia^R_j. \tag{A4}$$

The coefficients $a^R_j = a_j$, given in Eq. (D5) of Ref. [22]. Assuming $a^o_j = 0$ for $j < 0$, this recurrence allows for the calculation of all a^o_j. Note that this recurrence fails at $j = 1$, which represents the homogeneous solution to Eq. (A2). We can choose that coefficient to be anything.

The particular solution here is identical to the homogeneous solution to the fourth-order equation, given asymptotically in Eq. (3.8). We can use this asymptotic expansion for both situations.

On the horizon side, where the potential falls away exponentially, it is enough to use the expression in Eq. (3.20) and a sufficiently large and negative r_* starting location for integration. A Taylor expansion could be used if the starting location were farther from the horizon. The boundary conditions to the second-order homogeneous solutions are exactly analogous to those given in the odd-parity recurrence of Appendix D in Ref. [22]. The only difference is a change from 2 to 1 of the spin parameter in the potential.

[1] NASA, Lisa project office web site, http://lisa.nasa.gov.
[2] ESA, Next steps for lisa, http://sci.esa.int/science-e/www/object/index.cfm?fobjectid=48728.
[3] E. Poisson, A. Pound, and I. Vega, Living Rev. Relativity **14**, 7 (2011), http://relativity.livingreviews.org/Articles/lrr-2011-7/.
[4] A. Pound, Phys. Rev. D **81**, 124009 (2010).
[5] Y. Mino, M. Sasaki, and T. Tanaka, Phys. Rev. D **55**, 3457 (1997).
[6] T. C. Quinn and R. M. Wald, Phys. Rev. D **56**, 3381 (1997).
[7] L. Barack and A. Ori, Phys. Rev. D **61**, 061502 (2000).
[8] S. L. Detweiler and B. F. Whiting, Phys. Rev. D **67**, 024025 (2003).
[9] L. Barack and A. Ori, Phys. Rev. D **64**, 124003 (2001).
[10] L. Barack, Classical Quantum Gravity **26**, 213001 (2009).
[11] L. Barack and N. Sago, Phys. Rev. D **75**, 064021 (2007).
[12] L. Barack and N. Sago, Phys. Rev. Lett. **102**, 191101 (2009).
[13] L. Barack and N. Sago, Phys. Rev. D **81**, 084021 (2010).
[14] E. Poisson, in Proceedings of 5th Capra Meeting on Radiation Reaction in General Relativity, Penn State University, 2002 (unpublished).
[15] E. Rosenthal, Phys. Rev. D **73**, 044034 (2006).
[16] A. Pound, Phys. Rev. D **81**, 024023 (2010).
[17] C. Galley (private communication).
[18] E. E. Flanagan and T. Hinderer, Phys. Rev. Lett. **109**, 071102 (2012).
[19] L. Barack, A. Ori, and N. Sago, Phys. Rev. D **78**, 084021 (2008).
[20] S. Akcay, Phys. Rev. D **83**, 124026 (2011).
[21] N. Warburton, S. Akcay, L. Barack, J. R. Gair, and N. Sago, Phys. Rev. D **85**, 061501 (2012).
[22] S. Hopper and C. R. Evans, Phys. Rev. D **82**, 084010 (2010).
[23] N. Sago, H. Nakano, and M. Sasaki, Phys. Rev. D **67**, 104017 (2003).
[24] K. Thorne and A. Campolattaro, Astrophys. J. **149**, 591 (1967).
[25] F. Zerilli, Phys. Rev. D **2**, 2141 (1970).
[26] S. L. Detweiler and E. Poisson, Phys. Rev. D **69**, 084019 (2004).
[27] C. Misner, K. Thorne, and J. Wheeler, *Gravitation* (Freeman, San Francisco, 1973).
[28] C. Darwin, Proc. R. Soc. A **249**, 180 (1959).
[29] C. Cutler, D. Kennefick, and E. Poisson, Phys. Rev. D **50**, 3816 (1994).
[30] T. Regge and J. Wheeler, Phys. Rev. **108**, 1063 (1957).
[31] K. Martel and E. Poisson, Phys. Rev. D **71**, 104003 (2005).
[32] C. Cunningham, R. Price, and V. Moncrief, Astrophys. J. **224**, 643 (1978).
[33] K. Martel, Phys. Rev. D **69**, 044025 (2004).
[34] S. Chandrasekhar, *The Mathematical Theory of Black Holes*, The International Series of Monographs on Physics Vol. 69 (Clarendon, Oxford, 1983).
[35] D. V. Gal'tsov, J. Phys. A **15**, 3737 (1982).